Physica B 406 (2011) 575–578

Contents lists available at ScienceDirect

Physica B

journal homepage: www.elsevier.com/locate/physb

Extraction of important electrical parameters of CuO

T. Serin [a], A. Yildiz [b,*], Ş. Horzum Şahin [a], N. Serin [a]

[a] Department of Engineering Physics, Faculty of Engineering, Ankara University, 06100 Ankara, Turkey
[b] Department of Physics, Faculty of Science and Arts, Ahi Evran University, 40040 Kirsehir, Turkey

ARTICLE INFO

Article history:
Received 23 July 2010
Accepted 14 November 2010

Keywords:
CuO
Dip coating technique
Electrical parameters
Compensation ratio

ABSTRACT

Conductivity, X-ray diffraction (XRD), optical absorption and atomic force microscopy (AFM) measurements of CuO thin film were presented. Three distinct electrical conduction contributions with discrete characteristic activation energies were observed. The applicability of various theoretical models was considered to explain results on electrical transport. We extracted important electrical parameters of CuO, which might be useful for its gas sensor applications.

1. Introduction

There is a growing interest in the development of transition metal oxides in the literature of recent years. Especially, electrical properties of these materials have been studied extensively [1–5]. CuO is a p-type transition metal oxides semiconductor [6]. It has received considerable attention due to its great potential as a material for gas sensor applications [7–9].

Although the grain boundary (GB) transport properties give rise to important information on gas sensing properties, determination of the presence of different conduction mechanisms in CuO is still debatable. Therefore, understanding the charge transport can be important to improve sensitivity properties. One of the most important parameters related to the performance of gas sensors is the surface trap density (N_t) determining the Debye screening length (L_D) of the material. The data on the electrical parameter related to gas sensing properties should be provided to improve gas sensitivity. Decreasing N_t in transitional metal oxides is an effective way to enhance gas sensitivity. When L_D is about half the crystallite size (L), maximum sensitivity can be achieved [10]. The optimum sensitivity is obtained for small L, large L_D and relative low carrier concentration [10].

In this work, we aim at demonstrating the determination of electrical transport properties by processing the temperature dependence of conductivity of polycrystalline CuO, which might also help to interpret important electrical parameters for its gas sensor applications.

2. Experimental

In this work the starting solution for the deposition of copper oxide was prepared by dissolving copper acetate [$Cu(CH_3COO)_2 \cdot H_2O$] in ethanol. Afterwards lactic acid and triethylamine ($C_6H_{15}N$) were added to the resulting solution. The films were deposited by dip coating technique on glass substrates that were ultrasonically cleaned in de-ionized water and acetone (CH_3COCH_3, Merck) for 30 min. Film deposition was carried out in air at room temperature with a controlled speed of approximately 0.36 cm/s. After withdrawal, the substrate with the liquid film adhering to it is baked at 300 °C for 5 min in air. The above coating and baking processes were repeated to increase the thickness of the film. Finally the as-deposited films were annealed in air at 500 °C for 1 h.

The microstructure of the deposited films was investigated using an Inel-EQUINOX 1000 diffractometer. The radiation source, the wavelength and the scanning range 2θ of the diffractometer were CoK_α, 0.179 nm and 30–65°, respectively. The optical band gap of the films was calculated by means of UV–vis–NIR transmittance measurements performed by Shimadzu UV-3600 spectrophotometer in the spectral range 300–1500 nm.

The surface morphology of the films was also observed by a SPM Solver-PRO (NT-MDT) in semi-contact mode. The root-mean-square (RMS) values of surface roughness were estimated. The electrical conductivity measurements were carried out using Keithley 2420 programmable constant current source in a temperature range 125–365 K.

3. Results and discussion

The X-ray diffraction patterns for CuO film are shown in Fig. 1. The spectra show the well-resolved two diffraction peaks.

* Corresponding author. Tel.: +90 386 252 80 50; fax: +90 386 252 80 54.
E-mail address: yildizab@gmail.com (A. Yildiz).

0921-4526/$ - see front matter © 2010 Elsevier B.V. All rights reserved.
doi:10.1016/j.physb.2010.11.044

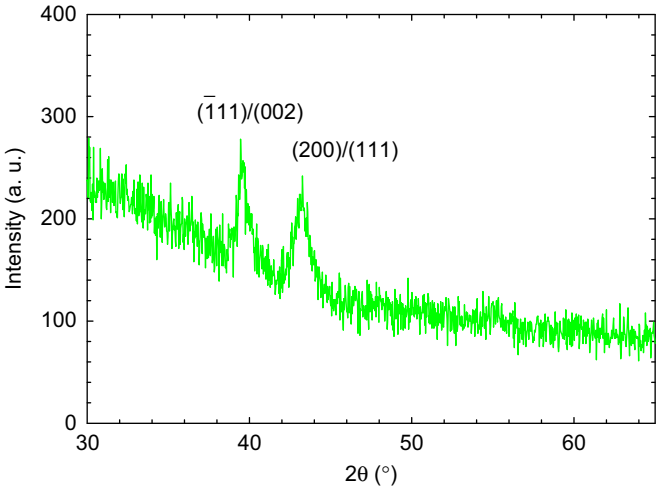

Fig. 1. XRD spectra of CuO.

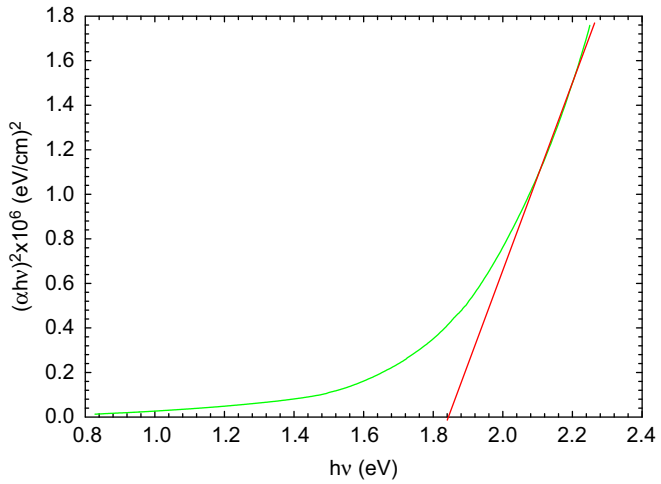

Fig. 2. Plot of $(\alpha h\nu)^2$ vs. $h\nu$ for CuO.

These peaks correspond to the reflection of the $(\bar{1}11)/(002)$ and $(200)/(111)$ planes of standard JCPDS data card of CuO [11]. Since all the peaks are sharp, it is evident that the films are polycrystalline in structure. The crystallite size for crystallites with $(200)/(111)$ plane was calculated using Scherrer's formula, neglecting peak broadening due to residual stresses in the films, $L=0.9\lambda/(\beta\cos\theta)$ where β is the broadening of diffraction line measured at half its maximum intensity in radians and λ is the wavelength of X-rays (0.179 nm). The calculated value of L is 14.9 nm.

The optical band gap of the film has been determined on the basis of UV–vis transmission measurements. For this, the fundamental absorption coefficient (α) was evaluated using $\alpha=(\ln T^{-1})/t$, where t is the film thickness and T is the transmittance. The value of absorption coefficient is of the order of 10^4 cm^{-1} supporting the direct band gap nature of the material. The nature of the direct allowed transition is determined using the relation

$$\alpha h\nu = A(h\nu - E_g)^{1/2} \quad (1)$$

where $h\nu$ is the photon energy, E_g is the optical band gap energy and A is a constant. The typical plot of $(\alpha h\nu)^2$ vs. $h\nu$ is depicted in Fig. 2, which indicates the presence of direct transition. The linear portion is extrapolated to $\alpha=0$ on the energy axis, which gives the band gap energy of 1.82 eV for the sample. It has been reported that the band gap of CuO can be changed to a wide range (1.75–2.15 eV) depending on the preparation conditions of CuO [12–15].

The surface morphology of the films is shown to be three- (3D) and two-dimensions (2D) in Fig. 3. AFM analysis showed that films are polycrystalline and have nano-grains. The root-mean-square (RMS) value of surface roughness was estimated as 4.04 nm.

In order to get a deeper insight into the conduction mechanisms, the temperature-dependent conductivity characteristics were performed in a temperature range of 125–365 K for the investigated sample. Fig. 4 shows the Arrhenius plot of the conductivity, σ, over whole temperature range. In particular, it is observable that no single law conduction can fit the entire curve of conductivity. The conductivity curve can be divided experimentally by operating in appropriately three regions, i.e. (i) $\Delta T_1=365$–295 K, (ii) $\Delta T_2=295$–200 K and (iii) $\Delta T_3=200$–125 K denoted by 'high temperatures', 'intermediate temperatures' and 'low temperatures', respectively.

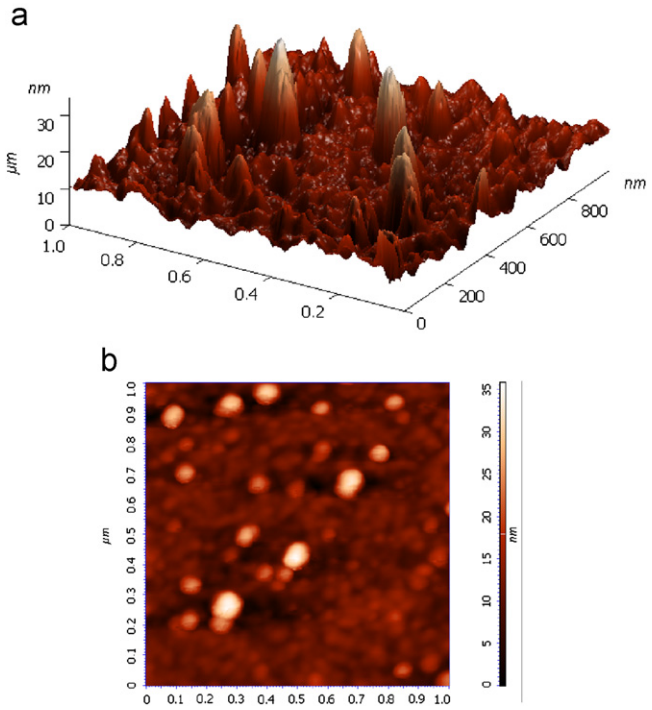

Fig. 3. (a) Three-dimensional (3D) and (b) two-dimensional (2D) AFM images of CuO.

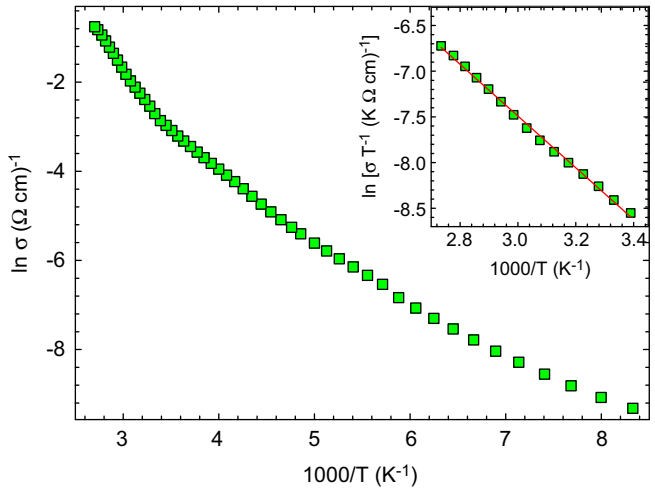

Fig. 4. Temperature dependence of conductivity plotted as $\ln(\sigma)$ vs. $10^3/T$ in a temperature range 125–365 K. Inset represents conductivity plotted as $\ln(\sigma T^{-1})$ vs. $10^3/T$. Solid lines are the best-fit lines with Eq. (2).

Since the polycrystalline film has crystallites joined at their surfaces via GB, the boundaries between crystallites play an important role in determining the conductivity of the polycrystalline film. In the polycrystalline materials, high densities of defects are expected at GBs, which are often charged with majority carriers. The charged states at the GBs create depleted regions, which also act as potential barriers [16,17]. Therefore, one can expect the GB model to explain the intermediate and high temperature data of the present polycrystalline sample. According to this model [16,17], the variation in electrical conductivity with temperature depends on whether the grains are fully depleted or partially depleted of charge carriers. Since the undoped CuO is a p-type material, we can suppose that the acceptor concentration is N_a. According to the GB model [18], a critical value of impurity concentration (N_a^*) can be defined. For $N_a < N_a^*$, the crystallites are entirely depleted, and Fermi level energy (E_F) becomes aligned with energy E_t (with respect to E_F at the interface). In this regime, conductivity can be written in the form [18]

$$\sigma = \left[\frac{L^2 e^2 N_v N_a v_c}{2k_B T(N_t - LN_a)}\right] \exp\left(-\frac{E_a}{k_B T}\right) \tag{2}$$

and v_c is the collection velocity [18]

$$v_c = \left(\frac{k_B T}{2\pi m^*}\right)^{1/2} \tag{3}$$

where e is the electron charge, k_B is Boltzmann's constant, m^* is the effective mass of charge carriers and N_v is the valance band effective density of states, which is described as

$$N_v = 2\left(\frac{2\pi m* k_B T}{h^2}\right)^{3/2} \tag{4}$$

where h is Planck's constant.

In the second case $N_a > N_a^*$, the grains are only partially depleted. Electrical conductivity can be expressed as [16,18]

$$\sigma = \left(\frac{Le^2 n v_c}{k_B T}\right) \exp\left(-\frac{E_a}{k_B T}\right) \tag{5}$$

where n is the electron concentration in neutral region of crystallites. In this regime, the activation energy (E_a) equals the barrier energy (E_b) at the boundary. E_b can be described as [16,18]

$$E_b = \frac{L^2 e^2 N_a}{8\varepsilon} \tag{6}$$

where ε is the low frequency dielectric constant. Applicability of the GB model involves many grain boundaries. This effect is examined by evaluation of the L_D in comparison with L. L_D is given as [17]

$$L_D = \sqrt{k_B T \varepsilon_0 \varepsilon / e^2 N_a} \tag{7}$$

where ε_0 is the dielectric constant of vacuum. If $L_D < L/2$, potential barriers exist in the GB region due to interface trap states [17]. If, however, L_D is larger than $L/2$, the conduction band becomes flat without the potential barrier [17]. Then carriers are transported without GB scattering.

In order to judge the comparative suitability of the above-mentioned two models given by Eqs. (2) and (5) fitted to our experimental data, we have calculated the values of the square of the linear correlation coefficient (χ^2). A comparatively high value of $\chi^2 = 0.999$ for the GB model confirms that this model is most suitable for explaining the conduction process in the intermediate and high temperature ranges of CuO. In the temperature ranges ΔT_1, the temperature dependence of the electrical conductivity is described by Eq. (2). The fully depleted crystallite formula (2) gives a well fit to the conductivity data for the studied sample in the considered temperature range (inset of Fig. 4). In Eq. (2), value of N_t (5.76×10^{12} cm^{-2}) is deduced from the straight line of the plot of $\ln(\sigma T^{-1})$ vs. $1000/T$. In Eq. (2), the value of effective mass (m^*) is $7.9m_0$ [6]. N_t is in excellent agreement with the reported values,

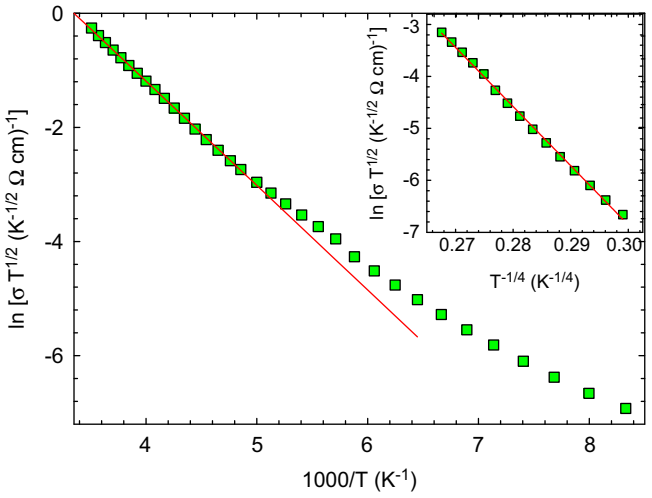

Fig. 5. Temperature dependence of conductivity plotted as $\ln(\sigma T^{1/2})$ vs. $10^3/T$. Solid lines are the best-fit lines with Eq. (5). Inset represents conductivity plotted as $\ln(\sigma T^{1/2})$ vs. $T^{-1/4}$. Solid lines are the best-fit lines with Eq. (8).

which is in the order of magnitude of 10^{12} for polycrystalline systems [16–18].

For the temperature range ΔT_2 (Fig. 5), the conductivity data are well fitted by Eq. (5), which indicates that electrical conduction is controlled by charge carriers trapped by partially depleted grains. According to the GB model [16–18], the carrier concentration increases with the decrease in temperature. This suggests that electrical conduction is controlled by charge carriers that are trapped by partially depleted grains in the intermediate temperatures. Estimating the value of ε as 12.3 for CuO [19], the value of the E_b can be calculated as 0.157 eV. Then, the value of N_a can be determined as 3.43×10^{18} cm^{-3}. Knowing the value of N_a, the value of the L_D was obtained as 2.13 nm. We noticed that the condition $L_D < L/2$, appropriate for the GB model is obeyed by the investigated sample. Therefore, the approach of analyzing the data using the GB model for the thermal activation of conductivity is valid for the investigated sample.

The conductivity below about 200 K deviates from the GB model (Fig. 5). The temperature dependence of electrical conductivity in the temperature range ΔT_3 is best described by Mott's variable range hopping (VRH) in which the expression for conductivity at low temperatures is given by [20]

$$\sigma = \sigma_{0,v} T^{-1/2} \exp(-T_0/T)^{1/4} \tag{8}$$

where

$$\sigma_{0,v} = \frac{3e^2 v}{(8\pi)^{1/2}} \left[\frac{\xi N(E_F)}{k_B}\right]^{1/2} \tag{9}$$

T_0 is a characteristic temperature coefficient that depends on the density of states $N(E_F)$ at the Fermi level in the form [20]

$$T_0 = \frac{18}{k_B \xi^3 N(E_F)} \tag{10}$$

where v is the typical phonon frequency and ξ is the localized state wave function, which represents the degree of localization of the electronic states in the impurity band. Inset of Fig. 5 represents the behavior of $\ln(\sigma T^{1/2})$ as a function of $T^{-1/4}$ according to the VRH model, following Eq. (8) in the 125 – 200 K temperature range. In the temperature range ΔT_3, the behavior is evidently linear ($\chi^2 = 0.999$); the slope of the linear fit leads to a value of $T_0 = 1.68 \times 10^8$ K, which corresponds to the $N(E_F) = 2.26 \times 10^{21}$ cm^{-3} eV^{-1}. The value of ξ was assumed to be in the same order as the Bohr radius ($a_B = 4\pi\varepsilon_0\varepsilon h^2/m*e^2$) for CuO. The value of T_0, which is a measure of disorder in the material, is significantly high due to high

compensation ratio ($k = N_d/N_a$ for p-type) [21]. Such a high T_0 value was also reported for Cu-doped $BaTiO_3$ polycrystals [22]. Obtained value of the $N(E_F)$ is close to that previously reported for various systems having the same origin [23,24].

In order to explain the observed hopping conduction through localized states near the Fermi level in the temperature range ΔT_3, we should consider the presence of intrinsic defects of CuO. CuO usually includes non-stoichiometry [6]. The presence of imperfections associated with polycrystalline films has an important role in the determination of electrical properties. Such defects lead to the formation of localized energy states in the forbidden band gap. A change in the transport mechanism from GB conduction to VRH conduction is expected at temperatures at which the carriers do not have sufficient energy to cross the potential barrier and transfer themselves into the crystallite by the process of thermionic emission [25].

There are two important hopping parameters: the hopping distance R, which depends upon the overlap of the wave functions, and the average hopping energy W can be determined using the following expressions [20]:

$$R = \left[\frac{9\xi}{8\pi N(E_F)k_BT}\right]^{1/4} \tag{11}$$

$$W = \frac{3}{4\pi R^3 N(E_F)} \tag{12}$$

The values of R and W were calculated to be 1 nm and 105 meV, respectively. These results are in good agreement with conductivity analyses in the frame of the VRH model [1,20].

Hopping conduction can be fulfilled only by donor–acceptor compensation. The knowledge of $N(E_F)$ allows us to calculate k, which characterizes the degree of disorder. In our case, high compensation is responsible for observation of the impurity band conduction. Normally, VRH conduction can be expected at very low temperatures. On the other hand, if a system is very heavily compensated, it is possible that the hopping regime can be observed in a wide temperature range. Finally, we can obtain the value of k and then the donor concentration (N_d) using an expression valid for a compensated material in case of $k > 0.5$ [26]

$$N(E_F) = (2\varepsilon/e^2)N_a^{2/3}(1-N_d/N_a)^{4/3} \tag{13}$$

Substituting the values of $N(E_F)$ and N_a in Eq. (13), the values of k and N_d can be determined as 0.88 and $3.43\times10^{18}\,\mathrm{cm}^{-3}$, respectively.

4. Conclusion

Conductivity, atomic force microscopy (AFM) and X-ray diffraction (XRD) measurements of CuO thin film were presented. Three distinct activation contributions with discrete characteristic activation energies were observed. The temperature dependence of electrical conductivity between 200 and 365 K indicated that electrical conductivity in the film was controlled by potential barriers caused by depletion of carriers at grain boundaries. The conductivity at low temperatures ($T < 200$ K) demonstrated VRH conduction. Important electrical parameters such as surface trap density, the Debye screening length, density of states at Fermi level and compensation ratio were determined.

Acknowledgements

This work was supported by the State of Planning Organization of Turkey under Grant no. 2001K120590 and the Ankara University BAP under Project number 2007-07-45-054. We would also like to thank Prof. Dr. Yusuf Kağan Kadıoğlu and Ms. Murat Yavuz for providing XRD and AFM measurements.

References

[1] A. Yildiz, S.B. Lisesivdin, M. Kasap, D. Mardare, J. Non-Cryst. Solids 354 (2008) 4944.
[2] A. Yildiz, S.B. Lisesivdin, M. Kasap, D. Mardare, Physica B 404 (2009) 1423.
[3] A. Yildiz, N. Serin, T. Serin, M. Kasap, Opt. Adv. Mater. Rapid Commun. 3 (2009) 1034.
[4] A. Yildiz, S.B. Lisesivdin, M. Kasap, D. Mardare, J. Mater. Sci: Mater. Electron 21 (2010) 692.
[5] T. Serin, A. Yildiz, N. Serin, N. Yıldırım, F. Özyurt, M. Kasap, J. Electron. Mater. 39 (2010) 1152.
[6] T. Ito, H. Yamaguchi, K. Okabe, T. Masumi, J. Mater. Sci. 33 (1998) 3555.
[7] M. Frietsch, F. Zudock, J. Goschnick, M. Bruns, Sensors Actuators B 65 (2000) 379.
[8] P. Samarasekara, N.T.R.N. Kumara, N.U.S. Yapa, J. Phys.: Condens. Matter 18 (2006) 2417.
[9] Z. Jiao, F. Chen, R. Su, X. Huang, W. Liu, J. Liu, Sensors 2 (2002) 366.
[10] F. Cosandey, G. Skandan, A. Singhal, JOM-e 52 (10) (2000). 〈http://www.tms.org/pubs/journals/JOM/0010/Cosandey/Cosandey-0010.html〉.
[11] JCPDS Card no 65-2309 (Monoclinic CuO).
[12] E.M. Alkoy, P.J. Kelly, Vacuum 79 (2000) 221.
[13] S.C. Ray, Sol. Energy Mater. Sol. Cells 68 (2001) 307.
[14] J.F. Pierson, A. Thobor-Keck, A. Billard, Appl. Surf. Sci. 210 (2003) 359.
[15] M. Nair, L. Guerrero, O. Arenas, P. Nair, Appl. Surf. Sci. 150 (1999) 143.
[16] J.Y.W. Seto, J. Appl. Phys. 46 (1975) 5247.
[17] J.W. Orton, M.J. Powel, Rep. Prog. Phys. 43 (1980) 1263.
[18] G. Baccarani, B. Ricco, G. Spandini, J. Appl. Phys. 49 (1978) 5565.
[19] W.Y. Ching, Y-N. Xu, K.W. Wong, Phys. Rev. B 40 (1989) 7684.
[20] N.F. Mott, E.A. Davis, Electronic Process in Non-Crystalline Materials, Clarendon, Oxford, 1979.
[21] A. Yildiz, S.B. Lisesivdin, H. Altuntas, M. Kasap, S. Ozcelik, Physica B 404 (2009) 4202.
[22] C Ang, Z Jing, Z. Yu, J. Phys.: Condens. Matter 11 (1999) 9703.
[23] A. Yildiz, N. Serin, T. Serin, M. Kasap, Jpn. J. Appl. Phys. 48 (2009) 111203.
[24] K. Dutta, S.K. De, J. Phys. D: Appl. Phys. 40 (2007) 734.
[25] M.M. Abdul-gader, M.A. Al-basha, K.A. Wishah, Int. J. Electron. 85 (1998) 21.
[26] B.I. Shklovskii, Sov. Phys. Semicond. 6 (1973) 1053.